

# Using a L-Band Weak-Resonant-Cavity FPLD for Subcarrier Amplitude Pre-Leveled 16-QAM-OFDM Transmission at 20 Gbit/s

Gong-Ru Lin, *Senior Member, IEEE, OSA*, Yu-Chieh Chi, Yi-Cheng Li, and Jyehong Chen

**Abstract**—A directly modulated and coherently injection-locked WRC-FPLD transmitter is preliminarily employed to perform the 16-QAM-OFDM data transmission by using an OFDM subcarrier amplitude pre-leveling technique. The maximum transmission bit-rate of 20-Gbit/s is reported by fusing the OFDM subcarrier pre-leveling with the coherent injection-locking techniques in such a directly modulated WRC-FPLD. Without pre-leveling the OFDM subcarrier, the coherently injection-locked L-band WRC-FPLD suppresses its mode-partition noise to improve the EVM of the 16-QAM-OFDM data only from 13.52% to 10.2%. The OFDM subcarrier pre-leveling effectively compensates the finite bandwidth and unflattened modulating response of the injection-locked WRC-FPLD to improve the transmission EVM and SNR performances. The received constellation plot reveals that the EVM and SNR of the back-to-back transmitted 16-QAM-OFDM data are significantly improved to 5.58% and 17 dB, respectively. With the use of both injection-locking and pre-leveling techniques, the directly 16-QAM-OFDM modulated WRC-FPLD transmitter can reach the FEC limited BER of  $3.8 \times 10^{-3}$  at a receiving power sensitivity of  $-10$  dBm. The OFDM subcarrier pre-leveling technique helps the WRC-FPLD to reduce the overall BER of 16-QAM-OFDM data by one order of magnitude, providing a minimum BER of  $4.5 \times 10^{-5}$  at a receiving power of  $-2$  dBm.

**Index Terms**—Amplitude pre-leveling, coherent injection-locking, direct modulation, FPLD, QAM-OFDM, subcarrier, transmission, weak-resonant-cavity.

## I. INTRODUCTION

SINCE 2006, the coherent optical orthogonal frequency division multiplexing (OFDM) [1], [2] has already emerged as a new-class of high capacity data transmission format to enable the high spectral usage within a finite bandwidth [3]–[5]. Versatile data modulation schemes based on different transmitters and modulators to facilitate the carry

of optical OFDM were considered and successively demonstrated [6]–[10]. At an early stage, the direct modulation of single-mode laser sources including the distributed feedback laser diodes (DFBLDs) [6], [7], the vertical-cavity surface emitting laser diodes (VCSELs) [8], [9], and the self-feedback controlled Fabry-Perot laser diodes (FPLDs) [10], etc. have been investigated to carry the optical OFDM formatted data-stream. Later on, the tunable laser injection-locked reflective semiconductor optical amplifiers (RSOAs) were also demonstrated to be the down-stream reusable optical OFDM transmitters [11], [12]. With the electronic data format using the M-ary quasi-amplitude-modulation (QAM) integrated with multi-subcarrier OFDM, some remarkable milestone works have been reported to achieve high-data-rate optical OFDM transmission within the past few years, such as the 32-QAM-OFDM (128 subcarriers) transmission based on a tunable laser injection-locked RSOA transmitter with a total data-rate as high as 10 Gbit/s demonstrated by Duong and co-workers [12], and the 16-QAM-OFDM (64 subcarriers) transmission carried by using a DFBLD with a total bit rate of up to 30 Gbit/s reported by Mori *et al.* [13], [14]. Lin *et al.* have demonstrated radio-on-fiber (ROF) OOK/OFDM system [15] and established the 60-GHz radio-over-fiber systems employing the 16-QAM-OFDM transmission of up to 28 Gbit/s [16]. More recently, the hybrid cable television and 16-QAM-OFDM in-building networks over SMF and GI-POF have also been reported [17].

In particular, some new data bit-loading or pre-scaling [18]–[20] techniques have also been considered to modify the formats carried by different subcarriers of the original M-QAM-OFDM data-stream. In view of previous works, most implementations were emphasized on the single-mode coherent sources, whereas the study on using the wavelength injection-locking transmitters made by partially coherent multi-mode sources was seldom discussed. Nowadays, these kinds of sources including the reflective semiconductor optical amplifier (RSOA) [21], [22] and the multi-mode Fabry-Perot laser diodes (FPLDs) [23]–[25] under wavelength injection-locked have been applicable to the broadband dense-wavelength-division-multiplexing (DWDM) passive optical networks (PON). Owing to the gradually increasing need on both data and channel capacities for local access networks in next-generation communication architecture, the technical fusion of potential transmitter candidates like the wavelength injection-locked FPLDs and new-class of data-formats like the M-QAM-N-OFDM is urgent. Some remarkable achievements

Manuscript received September 05, 2012; revised January 02, 2013; accepted January 15, 2013. Date of publication January 22, 2013; date of current version February 11, 2013. This work was supported in part by the National Science Council, Taiwan, and in part the Excellent Research Projects of National Taiwan University, Taiwan, under Grants NSC98-2221-E-002-023-MY3, NSC100-2221-E-002-156-MY3, and NSC101-2221-E-002-071-MY3.

G.-R. Lin, Y.-C. Chi, and Y.-C. Li are with the Graduate Institute of Photonics and Optoelectronics, and the Department of Electrical Engineering, National Taiwan University, Taipei 10617, Taiwan (e-mail: grlin@ntu.edu.tw).

J. Chen is with the Department of Photonics, National Chiao Tung University, Hsinchu 300, Taiwan.

Color versions of one or more of the figures in this paper are available online at <http://ieeexplore.ieee.org>.

Digital Object Identifier 10.1109/JLT.2013.2241733

were reported by research peers, such as using the optical carrier suppression and separation technique to generate upstream and downstream channels for a bi-directional WDM-PON [26], and a novel transmission system that seamlessly integrates the ROF with centralized optical OFDM based WDM-PON transmission was reported by Chang's group [27], [28]. Not long ago, a new class of FPLD with weak resonant cavity (WRC) and dense longitudinal mode features has emerged to be a potential candidate for the future WDM-PON applications [29], [30]. In comparison, the RSOA with broadband gain spectrum can serve as a colorless source for WDM-PON transmission after injection; however, the output coherence and modulation bandwidth of the RSOA based injection-locked transmitter is lower than that of the WRC-FPLD. In contrast, the WRC-FPLD further benefits from a higher SNR from its suppressed spontaneous emission noise when comparing with the RSOA output. These results facilitate the WRC-FPLD for noise-sensitive modulation such as the OFDM.

According to the definition of WDM-PON architecture with bi-directional down- and up-stream channels [31], [32], each channel utilizes different wavelength and the total channel bandwidth at C- and L-band is limited at around 30–35 nm. For a preset channel number of up to 32 with WDM channel spacing of 100 GHz, the limited gain bandwidth of the WRC-FPLD inevitably causes a band separation design for down- and up-stream WDM channels. In practical, the C-band WRC-FPLD is selected for down-stream and the L-band WRC-FPLD is selected for up-stream transmission in WDM-PON. However, most of the cost-effective FPLDs and WRC-FPLDs are packaged with TO-can module with a finite modulation bandwidth of less than 4–5 GHz [33], [34]. Unless the special designs on the package of the WRC-FPLD [35] can be performed to greatly improve the impedance mismatch and to release the effect from the parasitic circuitry [36], the modulation bandwidth cannot be easily enhanced to meet the demand of current M-QAM-N-OFDM with requested bandwidth of more than 4 GHz. The problem of finite modulation bandwidth for the TO-can packed FPLD has left as a bottleneck to be overcome at current stage. Currently, the WRC-FPLD is packaged in the cost-effective TO-46-can with its modulation bandwidth limited at 4–6 GHz. Even using a high-speed TO-can package with frequency bandwidth larger than 10 GHz, the inherent modulation bandwidth of the long-cavity WDC-FPLD could also induce another bottleneck for directly on-off-keying modulated PON application up to 40 Gbit/s. Nevertheless, with the combination of the directly 16-QAM OFDM modulation in a greatly reduced bandwidth of 10 GHz, the WRC-FPLD is no doubt a potential candidate for the next generation WDM/OFDM hybrid PON architecture.

In this work, a directly modulated and coherently injection-locked L-band FPLD with weak resonant cavity and dense longitudinal mode features (hereafter named as WRC-FPLD) is employed to carry the 16-QAM-OFDM data transmission at a total bit-rate of up to 20 Gbit/s. By individually pre-leveling the data-stream amplitude in each OFDM subcarrier to enhance the M-QAM-OFDM (N subcarriers) transmission, we demonstrate a breakthrough on promoting the allowable encoding bandwidth

as well as the total data bit-rate of the M-QAM-N-OFDM transmission carried by the L-band WRC-FPLD with a limited direct modulation bandwidth. The principles of the OFDM pre-leveling and the coherently wavelength injection-locking techniques in the WRC-FPLD with specific operating parameters are elucidated in detail, and the error vector magnitude (EVM) and the transmitted bit-error-rate (BER) responses of the L-band WRC-FPLD are demonstrated.

## II. EXPERIMENTAL SETUP

A TO-can packaged L-band WRC-FPLD with a typical ridge-waveguide structure consisting of a multi-quantum-well based active layer was employed as the transmitter, as shown in Fig. 1. In comparison with a traditional FPLD, the L-band WRC-FPLD cavity length was lengthened to 600  $\mu\text{m}$  so as to increase the mode spectral density, enabling at least one mode to be injection-locked within one DWDM channel with spacing as small as 200 GHz [37]. In particular, the front-end facet reflectance of the L-band WRC-FPLD was reduced to 1% such that the L-band WRC-FPLD remained a partial coherence with dense and weak longitudinal modes. Such a design also ensured that the power budget of the injection-locking operation can be greatly reduced [37], [38]. In experiment, the L-band WRC-FPLD exhibited a threshold current of 17 mA and a longitudinal mode spacing of 0.6 nm, which was wavelength injection-locked near its gain spectral peak at 1581 nm by using a single-mode wavelength-tunable laser (ANDO AQ4321D). The injection-locking with a power level of  $-3$  dBm was implemented through an optical circulator (JDSU, CIR-3-P-CL-2-1-FA) with an insertion loss of 0.7 dB. A polarization controller (PC) was used to control the polarization state injected into the L-band WRC-FPLD. The temperature of the L-band WRC-FPLD was controlled at 25°C with a residual fluctuation of smaller than 0.1°C to prevent the loose locking from wavelength drift of the longitudinal mode.

To enhance the modulation bandwidth and reduce the frequency chirp, such an injection-locked L-band WRC-FPLD was biased at 2 times the threshold and was directly modulated with the electrical 16-QAM-OFDM data with 108 subcarriers. The well beyond threshold operation of the L-band WRC-FPLD also helped to suppress the relative intensity noise (RIN) induced signal-to-noise ratio (SNR) degradation. The Fig. 2 illustrates the experimental setup of a coherently injection-locked and directly modulated L-band WRC-FPLD for 16-QAM-OFDM transmission. The 16-QAM-OFDM waveform in time domain was created by using a homemade MATLAB program with an inverse fast-Fourier transform (iFFT) size of 512, an OFDM subcarrier spacing of 46.8 MHz, a 16-QAM data bit of 187.4 Mbit/s, and a sampling rate of 24 GS/s. The 16-QAM-OFDM data stream was sent to the arbitrary waveform generator (AWG, Tektronix, 7122B) to generate the electrical 16-QAM-OFDM data stream with the same symbol rate of 24 GS/s. The output 16-QAM-OFDM data-stream with peak amplitude of 1.2  $V_{pp}$  at central frequency of 3 GHz was used to directly modulate the L-band WRC-FPLD through a bias-tee (Mini-Circuits ZX85-12G-S+). Moreover, the allowable subcarrier number, spacing and amplitude of the OFDM data were preset by the MATLAB program. After determining

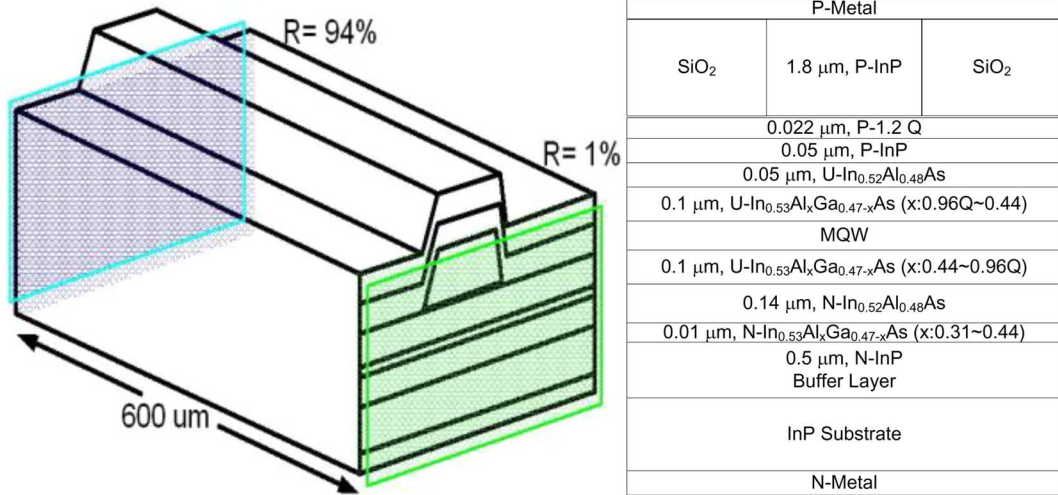


Fig. 1. The ridge-waveguide structure (left) and device configuration parameters of the WRC FPLD with 1% front-facet AR coating.

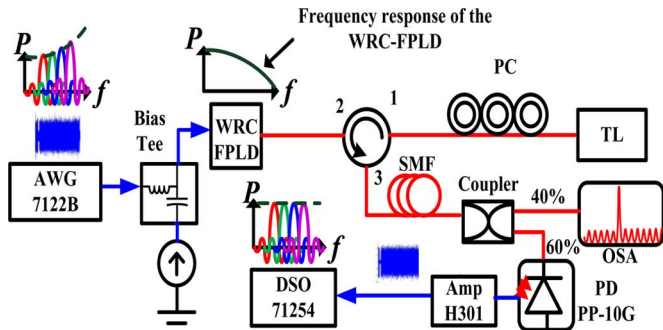


Fig. 2. The optical 16-QAM-OFDM data transmission set by using a directly modulated and coherently injection-locked L-band WRC-FPLD.

the frequency response of the L-band WRC-FPLD, the central frequency of the OFDM format can be decided around half modulation bandwidth of the L-band WRC-FPLD.

The lower output power of the L-band WRC-FPLD obtained at higher modulated frequency region was mainly attributed to the finite bandwidth of the TO-can package used to mount the L-band WRC-FPLD. An OFDM subcarrier pre-leveling technique was proposed to compensate the significant power decay beyond 3-dB frequency bandwidth. In contrast to optical OFDM data carried by the directly modulated L-band WRC-FPLD without any data processing, the optical 16-QAM-OFDM data used in this experiment was modified with its OFDM subcarrier peak pre-leveled by an exponential function of  $\sum_{m=-54}^{m=54} \exp(a \cdot f_{\text{sub},m})$  in which “ $a$ ” denoting the rising coefficient that effectively compensated the beyond-bandwidth attenuation to give a flattened signal in frequency domain. The “ $a$ ” factor represents the power-to-frequency slope of OFDM spectrum set from subcarrier number  $m = -54$  to  $m = +54$ . Owing to enlargement on the negative power-to-frequency slope in the modulation throughput power spectrum of the WRC-FPLD, the “ $a$ ” factor is employed to pre-level the OFDM subcarriers at different frequency for compensation. Both the performances of back-to-back and short-distance (through a 25-km single-mode-fiber) transmissions were characterized. The optical 16-QAM-OFDM data-stream carried

by the injection-locked L-band WRC-FPLD transmitter was received by a 10-Gbit/s p-i-n photodetector with a pre-amplifier (Nortel, PP-10 G). The optical receiver exhibited a relatively smooth modulation response and a cutoff frequency at 11 GHz. The received signal was linearly amplified by a 12.2-Gbit/s microwave amplifier (JDSU, H301) with a noise figure of 11 dB. Such a selected set of receiver and amplifier aimed to maintain the flattened gain response within a 3-dB frequency bandwidth ranged between 75 kHz and 10 GHz for the 16-QAM-OFDM data. Currently, a distributed sinusoidal-wave clock at frequency of 10 MHz is employed to the whole system including the carrier frequency generator, the arbitrary wave-form generator, and the real-time oscilloscope for clock synchronization. A frequency synchronization clock and carrier may be considered if RF up-conversion is needed. At last, the received 16-QAM-OFDM data was captured by using a digital oscilloscope (DSO, Tektronix, 71254) with a sampling rate of 50 GS/s, and was demodulated by using a MATLAB program to analyze the EVM and BER performances.

### III. RESULTS AND DISCUSSIONS

The selection of injection-locking power for the WRC-FPLD is mainly according to the relative intensity noise spectra of the WRC-FPLD injection-locked at different power levels, as shown in the following figure (see Fig. 3). The RIN peak of the injection-locked WRC-FPLD is up-shifted from 5.1 to 7.5 GHz with injection-locking power increasing from  $-12$  to  $-3$  dBm, which helps to improve the SNR within the OFDM modulation bandwidth of 5 GHz used in experiment.

After injection-locking, the threshold current of the L-band WRC-FPLD reduces from 17 to 12 mA, as shown in Fig. 4. The optical spectra of the L-band WRC-FPLD under free-running and injection-locking are shown in Fig. 5. The side-mode intensity of the L-band WRC-FPLD output is significantly suppressed by up to 40 dB after single-mode injection-locking at 1581 nm.

Although the difference between the biased and threshold currents of the L-band WRC-FPLD effectively increases to

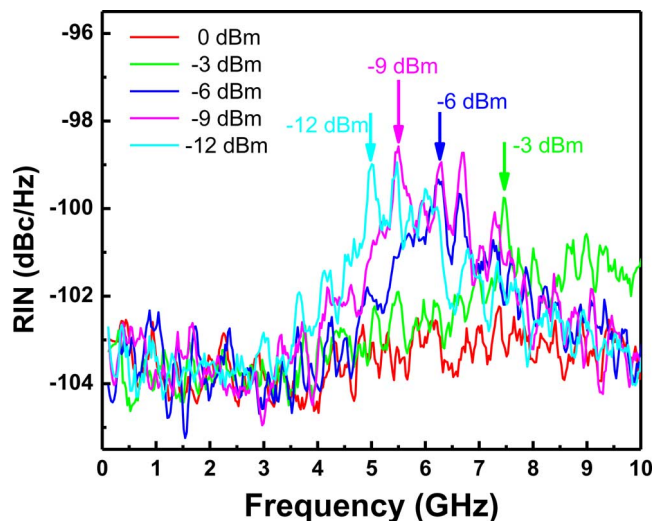


Fig. 3. RIN spectra of the WRC-FPLD injection-locked under different power levels.

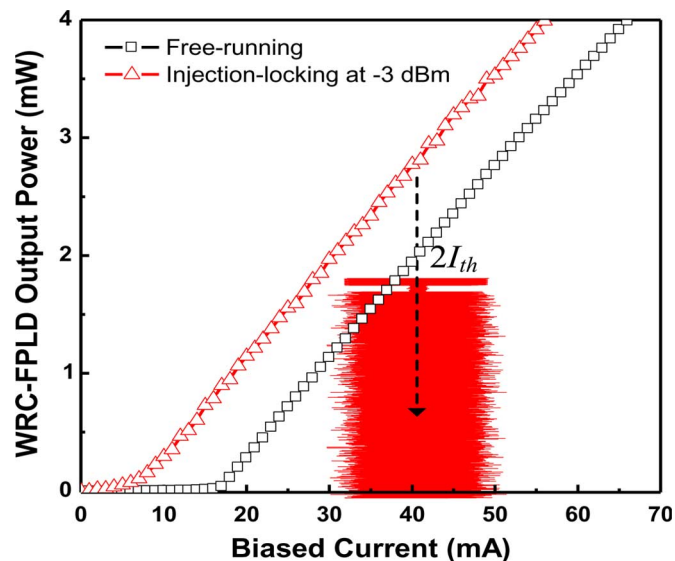


Fig. 4. P-I curves of the L-band WRC-FPLD without (black) and with (red) injection-locking.

up-shift the relaxation oscillation frequency, the direct modulation bandwidth slightly reduces due to the enlarged negative slope of the modulation response ( $dP_{out}/df$ ) decaying in frequency domain under strong injection-locking case.

As a result, the frequency responses of the directly modulated L-band WRC-FPLD without and with external injection-locking shown in Fig. 6 reveal that the modulation bandwidth slightly is increased from 6 to 6.5 GHz. In addition, the injection-locking further induces a small frequency dip of the L-band WRC-FPLD at 4–5 GHz. Not only the negative slope of the injection-locked L-band WRC-FPLD frequency response slightly increases, but also the output power of the directly modulated L-band WRC-FPLD attenuates to degrade the throughput. That is, the effects of the increased bias current and the enlarged injection level on the modulation bandwidth broadening of the WRC-FPLD could compensate each other. This is mainly attributed to the strong injection-locking which

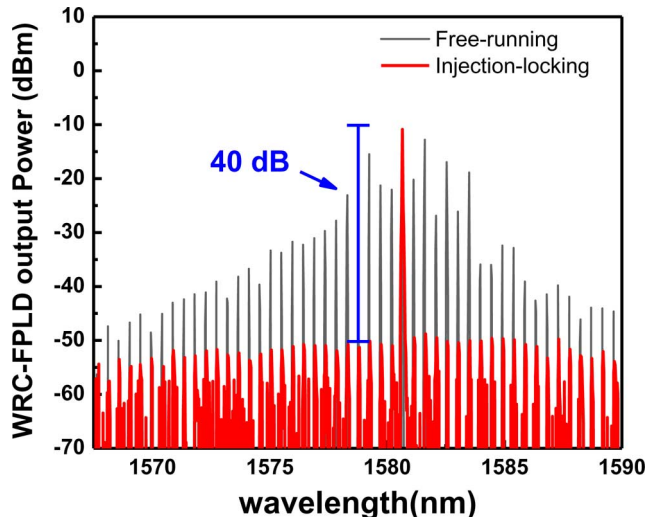


Fig. 5. Optical spectra of the L-band WRC-FPLD without (black) and with (red) injection locking.

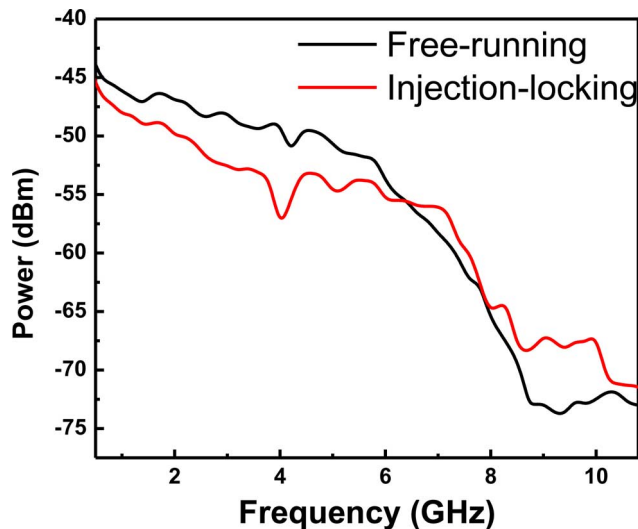


Fig. 6. Frequency response of the L-band WRC-FPLD without (black) and with (red) injection-locking.

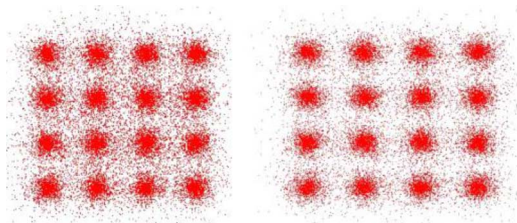


Fig. 7. The constellation plots of the 16-QAM-OFDM data carried by the free-running (left column) and injection-locked (right column) L-band WRC-FPLD transmitter.

preserves the wavelength and coherence but degrades the throughput of the L-band WRC-FPLD. To improve the transmission quality of the 16-QAM-OFDM data-stream, such a decayed throughput with an unexpected frequency dip should be compensated to make the L-band WRC-FPLD modulation response flattened.

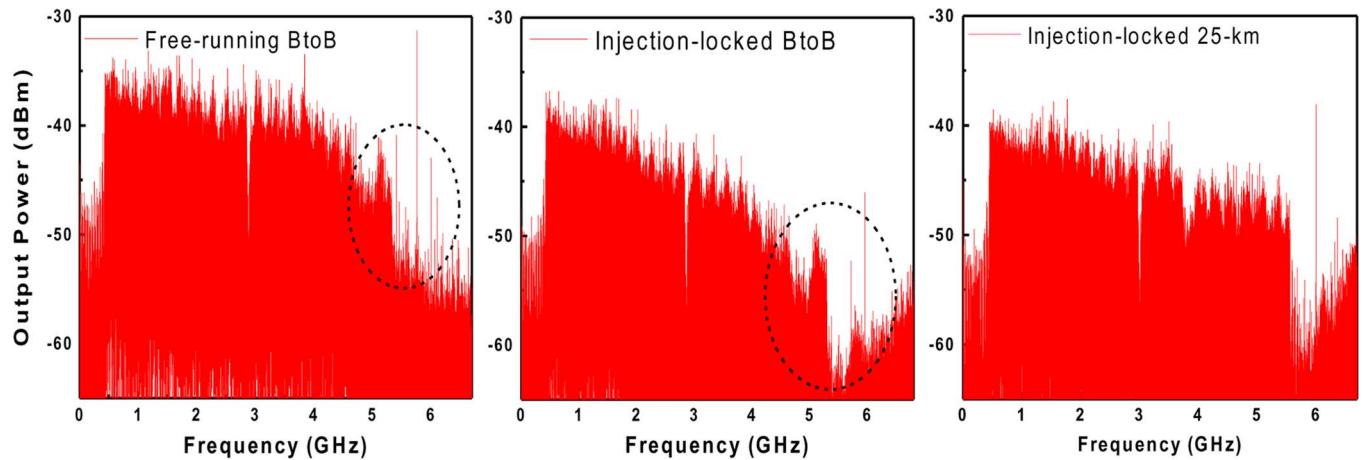


Fig. 8. The corresponding RF spectra of back-to-back and 25-km transmitted 16-QAM-OFDM data carried by the free-running (left column) and injection-locked (middle and right columns) L-band WRC-FPLD transmitter.

In experiment, each OFDM subcarrier demands to carry and transmit the maximal data rate, therefore the whole OFDM bandwidth is requested to occupy by the OFDM subcarriers as few as it can. Owing to the subcarrier spacing equation defined as  $\Delta f = \text{arbitrary waveform generator (AWG) sampling rate/FFT size}$ , the AWG sampling rate was increased to its upper limitation of 24 GS/s with a slightly non-integer resampling during demodulation. With a specified iFFT size of 512 set in our MATLAB program, the maximum data sampling rate to be hold in one OFDM subcarrier is 46.875 MS/s. After testing the capability of the WRC-FPLD transmitter, one OFDM subcarrier can expand its bandwidth to carry the 16-QAM data with a bit rate of up to 187.4 Mbit/s. In this case, the WRC-FPLD can hold up to 108 OFDM carriers with 16-QAM format in each subcarrier. Besides, the 16-QAM-OFDM data was captured by using a real-time oscilloscope (DSO, Tektronix, 71254) with the sampling rate fixed at 12.5, 25, 50, or 100 GS/s. The sampling rate of AWG and DSO are set identical to prevent from non-integer resampling. In this work, a Corning manufactured SMF (SMF-28™) with attenuation of  $<0.22$  dB/km at 1550 nm is employed for 25-km long transmission. The required bandwidth of the 20 Gbit/s 16-QAM-OFDM signal is 5 GHz. The cyclic prefix (CP) ratio is 1/32 without any pilot subcarriers. The resolution (bits) of the DAC in the AWG (Tectronix, 7122B) is 8 bit with a sampling rate of 24 GS/s. The resolution of the ADC is 8 bit in the DSO with a sampling rate of 25 GS/s.

Under direct modulation, the constellation plots and corresponding RF spectra of the transmitted 16-QAM-108-subcarrier-OFDM signal carried by the L-band WRC-FPLD at free-running and injection-locking cases are depicted in Figs. 7 and 8. In contrast to the EVM of 13.52% observed from the received 16-QAM-108-subcarrier-OFDM data carried by the L-band WRC-FPLD at free-running case, the relatively clear constellation plot with an EVM of 10.2% for the same data carried by the injection-locked L-band WRC-FPLD is obtained. Although the slope of the 16-QAM-OFDM signal carried by the L-band WRC-FPLD under injection-locking is tilted as compared to that under free-running case (see Fig. 8), the injection-locking induced noise suppression effect is positively contributed to the transmission performance of the

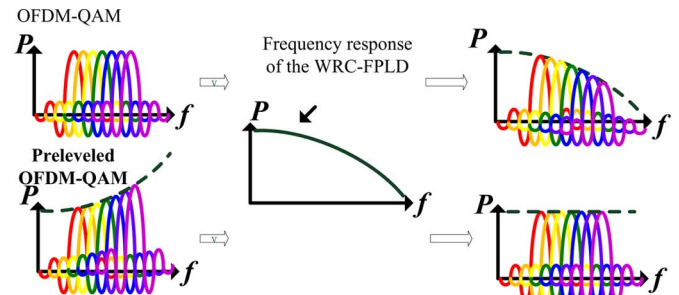


Fig. 9. The operating principle of the L-band WRC-FPLD directly modulated with a pre-leveled M-QAM-OFDM data for improving the transmission quality.

16-QAM-OFDM data. That is, the injection-locking essentially suppresses the phase incoherence and the intensity fluctuation of the L-band WRC-FPLD output, thus reducing both phase and amplitude errors to provide a clear constellation plot with decreasing EVM. However, the decayed and dipped response of the directly modulated L-band WRC-FPLD at high frequency region is clearly seen in Fig. 8, which still plays an important role to constrain the SNR as well as BER performance of the received 16-QAM-OFDM data. To improve this drawback, an OFDM subcarrier pre-leveling technique is proposed, which is introduced to compensate the imperfect direct modulation response inherently accompanied with the injection-locking L-band WRC-FPLD.

The operation principle of the L-band WRC-FPLD directly modulated with a pre-leveled M-QAM-OFDM (with  $N$  subcarriers) data for improving the transmission performance is illustrated in Fig. 7. In comparison with the traditional compensation scheme for properly decoding the M-QAM-OFDM data, the proposed OFDM subcarrier pre-leveling technique only take into account the analog modulation response of the L-band WRC-FPLD transmitter, which flattens the modulation response by multiplying with a rising exponential function  $\sum_{m=-54}^{m=54} \exp(af_{\text{sub},m})$ . The OFDM subcarrier pre-leveling technique emphasizes on maintaining the higher SNR of the transmitted M-QAM-OFDM data via the amplitude compensation of the transmitter response. This approach remits the need of the pre-transmission and post-compensation procedures,

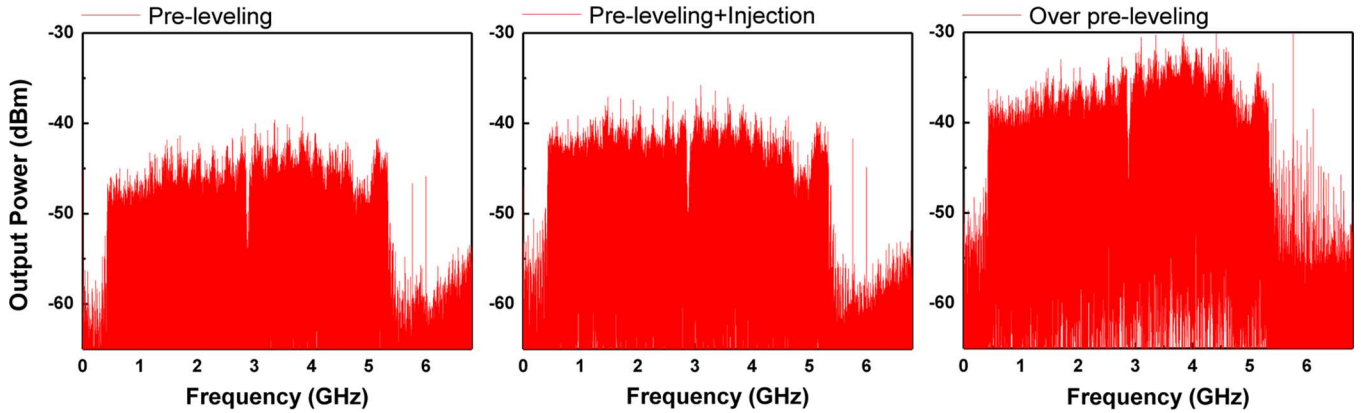


Fig. 10. The constellation plots (upper) and corresponding RF spectra (lower) for the 16-QAM-108-subcarrier-OFDM signal carried by the directly modulated L-band WRC-FPLD at free-running and pre-leveling (left), injection-locking and pre-leveling (middle), injection-locking and over-amplitude pre-leveling (right) cases.

and the M-QAM-OFDM transmission performance can be optimized when the analog modulation response is flattened.

As illustrated in Fig. 9, each of the OFDM subcarrier amplitude is pre-leveled in the MATLAB program according to the measured frequency response curve and slope of the L-band WRC-FPLD shown in Fig. 6. By directly modulating the L-band WRC-FPLD with such a pre-leveled M-QAM-OFDM data, the degraded frequency response is fixed so as to improve EVM and SNR of the 16-QAM data transmitted in all 108 OFDM subcarriers. The corresponding RF spectra for the directly modulated L-band WRC-FPLD at the free-running and pre-leveling case, the injection-locking and pre-leveling case, and the injection-locking and over-amplitude pre-leveling case are shown in Fig. 10. Among them, the injection-locked L-band WRC-FPLD modulated with a subcarrier pre-leveled OFDM data exhibits the most flattened response (see middle of Fig. 10).

By using the OFDM subcarrier pre-leveling technique on the directly modulated L-band WRC-FPLD even without injection-locking, the constellation plot of the transmitted 16-QAM-OFDM data shown in Fig. 13 significantly reduces its EVM from 13.52% to 9.1%. After wavelength injection-locking and directly modulated with a subcarrier pre-leveled 16-QAM and 108-subcarrier OFDM data, the L-band WRC-FPLD not only exhibits a coherently single-longitudinal-mode behavior with an enlarged side-mode suppressing ratio, but also provides an EVM as low as 5.58% for the transmitted 16-QAM-OFDM data. The corresponding SNR remains as high as 17 dB, which is already beyond the criterion of  $\text{SNR} = 15.2$  dB for obtaining a BER of  $3.8 \times 10^{-3}$  (leading to the error-free data communication standard after forward error correction process). The BER is calculating by using the formula of  $\text{BER} = 0.375 \cdot \text{erfc}(\sqrt{\text{SNR}}/10)$  according to the related [39].

The subcarrier-to-subcarrier intermixing interference (SSII) [40] at high frequency is much higher than that at lower frequency, which leads to a requirement on the higher SNR for the high frequency subcarriers as compared the low frequency subcarriers. In our case, the SNR obtained at different OFDM subcarriers under injection-locking and injection-locking+pre-leveling conditions are compared in Fig. 11. Although the SNR of low frequency subcarriers after

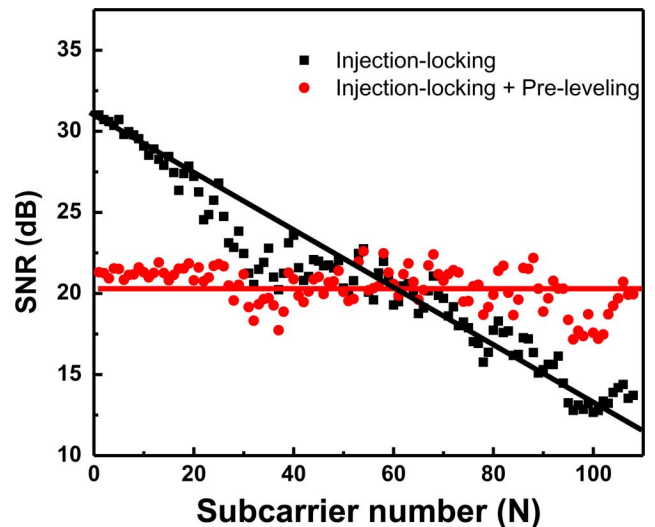


Fig. 11. SNR of 16-QAM data stream carried at each subcarrier after transmission by WRC-FPLD under injection-locking (black) and injection-locking + pre-leveling (red) conditions.

pre-leveling is lower than that without pre-leveling, the SNR of high frequency subcarriers is significantly improved. The average SNR obtained under injection-locking+pre-leveling operations are above 21 dB. Moreover, the theoretical BER of each subcarrier is calculated from SNR, which is shown in Fig. 12. Under pre-leveling, the maximum BER is further reduced from  $2.1 \times 10^{-2}$  to  $5 \times 10^{-4}$ . The pre-leveled OFDM modulation enables the injection-locked WRC-FPLD based transmitter to send data at higher bit rates over the subcarriers at frequencies near the bandwidth limitation, so as to improve the throughput and ensure an reduced BER of data transmitted by each subcarrier simultaneously.

In addition, the slope of the pre-leveled 16-QAM-OFDM data must be properly controlled to avoid the over compensation. In right part of Fig. 13, the over compensation inevitably leads to a noisy constellation plot with a degrading SNR observed at high-frequency RF spectrum of the transmitted M-QAM-OFDM data. As a result, the directly modulated

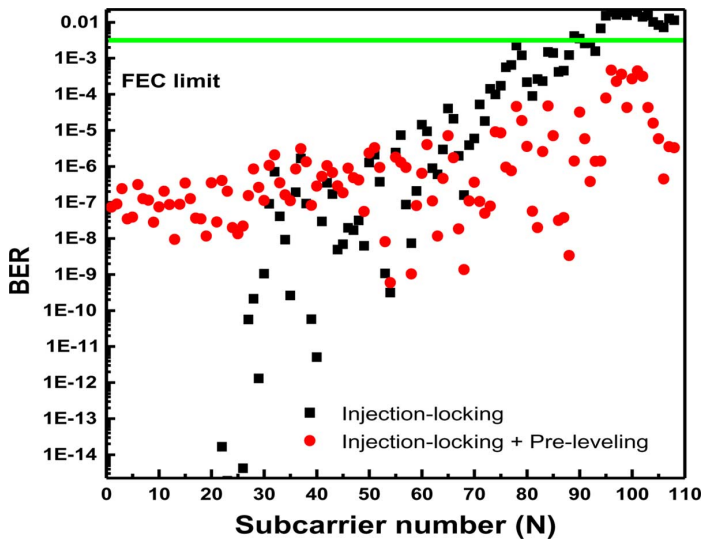


Fig. 12. Calculated BER of 16-QAM data stream carried at each subcarrier after transmission by WRC-FPLD under injection-locking (black) and injection-locking+pre-leveling (red) conditions.

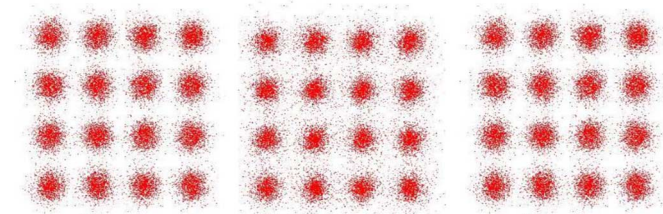


Fig. 13. The constellation plots for the 16-QAM-108-subcarrier-OFDM signal carried by the directly modulated L-band WRC-FPLD at free-running and pre-leveling (left), injection-locking and pre-leveling (middle), injection-locking and over-amplitude pre-leveling (right) cases.

L-band WRC-FPLD greatly improves its capability and transmission performance after injection-locking and pre-leveling processes, which can carry the 16-QAM-OFDM data with a total bit rate of up to 20.25 Gbit/s, as shown in Fig. 14. Under back-to-back transmission, the directly 16-QAM-OFDM modulated L-band WRC-FPLD without injection-locking reveals a BER as large as  $10^{-2}$  at receiving power of  $-10$  dBm. The BER is saturated at  $6.3 \times 10^{-3}$  even by increasing the power level of up to  $-3$  dBm. Without employing the OFDM subcarrier pre-leveling, the coherent injection-locking of the L-band WRC-FPLD further reduces the BER to  $10^{-3}$  at same receiving power sensitivity. The BER of the QAM-OFDM transmission is improved because the intensity fluctuation is minimized by reducing the mode-partition noise in the L-band WRC-FPLD, and the phase noise reduction is also enhanced by the coherent injection-locking.

With the use of both injection-locking and pre-leveling techniques, the receiving power sensitively for obtaining a FEC limited  $-\log(\text{BER})$  of 2.4 (or a BER of  $3.8 \times 10^{-3}$ ) [41], [42] can be significantly reduced to  $-10$  dBm, and the BER of  $<10^{-4}$  can be observed from the directly 16-QAM-OFDM modulated L-band WRC-FPLD at a receiving power of  $-6$  dBm. The lowest BER of  $4 \times 10^{-5}$  is reached by increasing the receiving power to  $-2$  dBm. With pre-leveling, the receiving

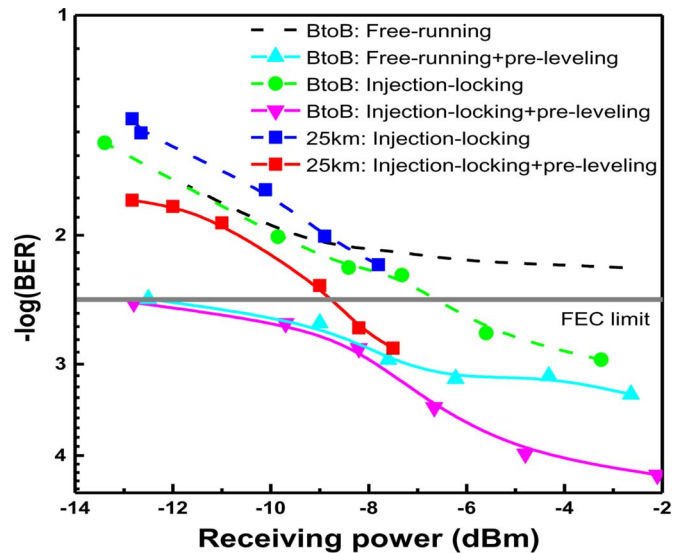


Fig. 14. Back-to-back and 25-km transmitted BER analyses of the original (dashed) and pre-leveled (solid) 16-QAM-108-subcarrier-OFDM data-streams carried by the directly modulated L-band WRC-FPLD at free-running (square) and injection-locking (circle) conditions.

power improved by  $-1.5$  dB at the same BER set by FEC limit. Even with pre-leveling and injection-locking, the lowest achievable BER of  $1 \times 10^{-3}$  achieved with a receiving power enlarged to  $-7$  dBm is observed after 25-km transmission. An overall improvement on the BER performance by one order of magnitude can be obtained with the use of the OFDM subcarrier pre-leveling technique. Note that the OFDM subcarrier pre-leveling technique plays a more important role than the injection-locking technique on improving the transmission EVM and SNR performances of the 16-QAM-OFDM data carried within the modulation frequency bandwidth of the L-band WRC-FPLD.

The chirp value of the directly on-off-keying modulated WRC-FPLD at different injection-locking powers has been reported previously [37]. Owing to the linear dispersion compensation by single-mode fiber, the peak-to-peak chirp after 25-km transmission can be reduced from 11 to 9 GHz by enlarging the injection-locking power from  $-12$  to  $-3$  dBm. Nevertheless, it is relatively difficult to real-time measure the chirp dynamics of transmitters under the direct modulation of OFDM format. Therefore, the aforementioned results may provide a comparable chirp data (assuming that the maximum frequency chirps for OOK and OFDM are comparable except their different duration in time domain). In comparison with the commercial laser diode which is biased at same condition of twice the threshold current, the WRC-FPLD could result in a relatively low chirp with maintained on/off extinction ratio. That is, the further chirp reduction relies strictly on either the high bias or the intense injection-locking [43] of the WRC-FPLD. For the unified colorless transmitters such as WRC-FPLDs, the wavelength injection-locking is mandatory to provide a coherent single-mode transmitter [44] for future DWDM application. Even though, the injection-locking inevitably tilts the modulation response in frequency domain to degrade the throughput of the L-band WRC-FPLD, which

needs to be effectively compensated via the proposed OFDM subcarrier pre-leveling technique. The experimental results elucidate that the fusion of wavelength injection-locking and subcarrier pre-leveling techniques can essentially preserve the SNR and improve the BER of the transmitted 16-QAM-OFDM data located at nearly the marginal frequency bandwidth region of the directly modulated WRC-FPLD.

#### IV. CONCLUSION

By pre-leveling the data-stream amplitude in each OFDM subcarrier, a coherently injection-locked and directly modulated WRC-FPLD has been demonstrated to perform the 16-QAM-OFDM transmission at a total bit-rate of up to 20 Gbit/s. The principles of the OFDM subcarrier pre-leveling and the wavelength injection-locking techniques for the L-band WRC-FPLD with specific operating parameters are elucidated. The EVM, SNR, and BER performances of the directly modulated L-band WRC-FPLD transmitter without and with the OFDM subcarrier pre-leveling and coherent wavelength injection-locking techniques are compared. Although the negative slope of the modulation response for the injection-locked L-band WRC-FPLD is enlarged as compared to that of the same device under free-running case, the EVM of the received 16-QAM-OFDM data is improved from 13.52% to 10.2%, because the intensity fluctuation is suppressed by reducing mode-partition and phase noises of the L-band WRC-FPLD under coherent injection-locking condition.

With the aid of OFDM subcarrier pre-leveling, the decayed and dipped response of the directly modulated and injection-locked L-band WRC-FPLD at high frequency region can be effectively compensated. This provides the further improved EVM and SNR of 5.58% and 17 dB, respectively. It is mandatory to address that the OFDM subcarrier pre-leveling technique plays a more important role than the injection-locking technique on improving the transmission EVM and SNR performances. Under back-to-back transmission with the coherently injection-locked and directly modulated L-band WRC-FPLD, the receiving power sensitivity required for decoding the 16-QAM-OFDM data at a FEC limited BER of  $3.8 \times 10^{-3}$  is significantly reduced to  $-10$  dBm. The combination of both injection-locking and pre-leveling techniques essentially helps to obtain a BER of smaller than  $4 \times 10^{-5}$  at a receiving power of  $-2$  dBm. No matter free-running or injection-locking case, an overall improvement on the BER performance by one order of magnitude can be obtained with the use of the OFDM subcarrier pre-leveling technique. The fusion of wavelength injection-locking and subcarrier pre-leveling techniques is mandatory for the directly 16-QAM-OFDM modulated L-band WRC-FPLD, which can effectively preserve the SNR and improve the BER performance of the carried M-QAM-OFDM data located at nearly the marginal frequency bandwidth region of the L-band WRC-FPLD transmitter.

#### REFERENCES

- [1] W. Shieh and C. Athaudage, "Coherent optical orthogonal frequency division multiplexing," *Electron. Lett.*, vol. 42, no. 10, pp. 587–589, May 2006.
- [2] W. Shieh, H. Bao, and Y. Tang, "Coherent optical OFDM: Theory and design," *Opt. Exp.*, vol. 16, no. 2, pp. 841–859, Jan. 2008.
- [3] J. Armstrong, "OFDM for optical communications," *J. Lightw. Technol.*, vol. 27, no. 3, pp. 189–204, Feb. 2009.
- [4] A. J. Lowery, "Fiber nonlinearity pre- and post-compensation for long-haul optical links using OFDM," *Opt. Exp.*, vol. 15, no. 20, pp. 12965–12970, Oct. 2007.
- [5] S. L. Jansen, I. Morita, T. C. W. Schenk, N. Takeda, and H. Tanaka, "Coherent optical 25.8-Gb/s OFDM transmission over 4160-km SSMAF," *J. Lightw. Technol.*, vol. 26, no. 1, pp. 6–15, 2008.
- [6] J. M. Tang, P. M. Lane, and K. A. Shore, "High-speed transmission of adaptively modulated optical OFDM signals over multimode fibers using directly modulated DFBs," *J. Lightw. Technol.*, vol. 24, no. 1, pp. 429–441, Jan. 2006.
- [7] X. Q. Jin, R. P. Giddings, E. Hugues-Salas, and J. M. Tang, "Real-time demonstration of 128-QAM-encoded optical OFDM transmission with a 5.25 bit/s/Hz spectral efficiency in simple IMDD systems utilizing directly modulated DFB lasers," *Opt. Exp.*, vol. 17, no. 22, pp. 20484–20493, Oct. 2009.
- [8] E. Hugues-Salas, R. P. Giddings, X. Q. Jin, J. L. Wei, X. Zheng, Y. Hong, C. Shu, and M. J. Tang, "Real-time experimental demonstration of low-cost VCSEL intensity-modulated 11.25 Gb/s optical OFDM signal transmission over 25 km PON systems," *Opt. Exp.*, vol. 19, no. 4, pp. 2979–2988, Feb. 2011.
- [9] A. Schimpf, D. Bucci, and B. Cabon, "Optimum biasing of VCSEL diodes for all-optical up-conversion of OFDM signals," *J. Lightw. Technol.*, vol. 27, no. 16, pp. 3484–3489, Aug. 2009.
- [10] C. H. Yeh, C. W. Chow, Y. F. Wu, F. Y. Shih, and S. Chi, "Using Fabry-Perot laser diode and reflective semiconductor optical amplifier for long reach WDM-PON system," *Opt. Commun.*, vol. 284, no. 21, pp. 5148–5152, Oct. 2011.
- [11] R. P. Giddings, E. Hugues-Salas, X. Q. Jin, J. L. Wei, and J. M. Tang, "Experimental demonstration of real-time optical OFDM transmission at 7.5 Gb/s Over 25-km SSMF using a 1-GHz RSOA," *IEEE Photon. Technol. Lett.*, vol. 22, no. 11, pp. 745–747, Jun. 2010.
- [12] T. Duong, N. Genay, P. Chanclou, B. Charbonnier, A. Pizzinat, and R. Brenot, "Experimental demonstration of 1 GHz RSOA using adaptively modulated optical OFDM for WDM-PON single fiber architecture," in *Proc. 34th ECOC*, 2008, vol. 7, pp. 39–49.
- [13] Y. Mori, C. Zhang, K. Igarashi, K. Katoh, and K. Kikuchi, "Unrepeated 200-km transmission of 40-Gbit/s 16-QAM signals using digital coherent optical receiver," *Opt. Exp.*, vol. 17, no. 3, pp. 1435–1441, Feb. 2009.
- [14] J. M. Tang and K. Alan, "30-Gb/s signal transmission over 40-km directly modulated DFB-laser-based single-mode-fiber links without optical amplification and dispersion compensation," *J. Lightw. Technol.*, vol. 24, no. 6, pp. 2318–2326, Jun. 2006.
- [15] C.-T. Lin, Y.-M. Lin, J. Chen, S.-P. Dai, P.-T. Shih, P.-C. Peng, and S. Chi, "Optical direct-detection OFDM signal generation for radio-over-fiber link using frequency doubling scheme with carrier suppression," *Opt. Exp.*, vol. 16, no. 9, pp. 6056–6063, Apr. 2008.
- [16] C.-T. Lin, J. Chen, P.-T. Shih, W.-J. Jiang, and S. Chi, "Ultra-high data-rate 60 GHz radio-over-fiber systems employing optical frequency multiplication and OFDM formats," *J. Lightw. Technol.*, vol. 28, no. 16, Aug. 2010.
- [17] H.-C. Peng, H.-S. Su, I. H.-H. Lu, C.-Y. Li, P.-C. Peng, S.-H. Wu, and C.-H. Chang, "Hybrid CATV/16-QAM OFDM in-building networks over SMF and GI-POF transport," *Opt. Exp.*, vol. 19, no. 10, pp. 9575–9581, May 2011.
- [18] Q. Yang, W. Shieh, and Y. Ma, "Bit and power loading for coherent optical OFDM," *IEEE Photon. Technol. Lett.*, vol. 20, no. 15, pp. 1305–1307, Aug. 2008.
- [19] H. Ochiai, "Performance analysis of peak power and band-limited OFDM system with linear scaling," *IEEE Trans. Wireless Commun.*, vol. 2, no. 5, pp. 1055–1065, Sep. 2003.
- [20] A. Ng'oma, C.-T. Lin, L.-Y. Wang He, W.-J. Jiang, F. Annunziata, J. Chen, P.-T. Shih, J. George, M. Sauer, and S. Chi, "31 Gbps RoF system employing adaptive bit-loading OFDM modulation at 60 GHz," in *Proc. OFC*, 2011, Paper OWT7.
- [21] K. Y. Cho, Y. Takushima, and Y. C. Chung, "10-Gb/s operation of RSOA for WDM PON," *IEEE Photon. Technol. Lett.*, vol. 20, no. 18, pp. 1533–1535, Sep. 2008.
- [22] C. W. Chow, C. H. Yeh, C. H. Wang, F. Y. Shih, and S. Chi, "Signal remodulation of OFDM-QAM for long reach carrier distributed passive optical networks," *IEEE Photon. Technol. Lett.*, vol. 21, no. 11, pp. 715–717, Jun. 2009.



- [23] G.-R. Lin, H. L. Wang, G. C. Lin, Y. H. Huang, Y. H. Lin, and T. K. Cheng, "Comparison on injection-locked Fabry-Perot laser diode with front-facet reflectivity of 1% and 30% for optical data transmission in WDM-PON system," *J. Lightw. Technol.*, vol. 27, no. 14, pp. 2779–2785, Jul. 2009.
- [24] Z. Xu, Y.-J. Wen, W.-D. Zhong, C.-J. Chae, X.-F. Cheng, Y. Wang, C. Lu, and J. Shankar, "High-speed WDM-PON using CW injection-locked Fabry-Pérot laser diodes," *Opt. Exp.*, vol. 15, no. 6, pp. 2953–2962, Mar. 2007.
- [25] G.-R. Lin, T.-K. Cheng, Y.-H. Lin, G.-C. Lin, and H.-L. Wang, "A weak-resonant-cavity Fabry-Perot laser diode with injection-locking mode number-dependent transmission and noise performances," *J. Lightw. Technol.*, vol. 28, no. 9, pp. 1349–1355, May 2010.
- [26] O. Akanbi, J. Yu, and G.-K. Chang, "A new scheme for bidirectional WDM-PON using upstream and downstream channels generated by optical carrier suppression and separation technique," *IEEE Photon. Technol. Lett.*, vol. 18, no. 2, pp. 340–342, Jan. 2006.
- [27] J. Yu, M.-F. Huang, D. Qian, L. Chen, and G.-K. Chang, "Centralized lightwave WDM-PON employing 16-QAM intensity modulated OFDM downstream and oofdm modulated upstream signals," *IEEE Photon. Technol. Lett.*, vol. 20, no. 18, pp. 1545–1547, Sep. 2008.
- [28] L. Chen, J. G. Yu, S. Wen, J. Lu, Z. Dong, M. Huang, and G. K. Chang, "A novel scheme for seamless integration of ROF with centralized lightwave OFDM-WDM-PON system," *J. Lightw. Technol.*, vol. 27, no. 14, pp. 2786–2791, Jul. 2009.
- [29] G.-R. Lin, Y.-S. Liao, Y.-C. Chi, H.-C. Kuo, G.-C. Lin, H.-L. Wang, and Y.-J. Chen, "Long-cavity Fabry-Perot laser amplifier transmitter with enhanced injection-locking bandwidth for WDM-PON application," *J. Lightw. Technol.*, vol. 28, no. 20, pp. 2925–2932, Oct. 2010.
- [30] Y.-H. Lin, C.-J. Lin, G.-C. Lin, and G.-R. Lin, "Saturated signal-to-noise ratio of up-stream WRC-FPLD transmitter injection-locked by down-stream data-erased ASE carrier," *Opt. Exp.*, vol. 19, no. 5, pp. 4067–4075, Feb. 2011.
- [31] Z. Xu, Y. J. Wen, W.-D. Zhong, C.-J. Chae, X.-F. Cheng, Y. Wang, C. Lu, and J. Shankar, "High-speed WDM-PON using CW injection-locked Fabry-Pérot laser diodes," *Opt. Exp.*, vol. 15, no. 6, pp. 2953–2962, Mar. 2007.
- [32] A. Banerjee, Y. Park, F. Clarke, H. Song, S. Yang, G. Kramer, K. Kim, and B. Mukherjee, "Wavelength-division-multiplexed passive optical network (WDM-PON) technologies for broadband access: A review [Invited]," *J. Opt. Commun. Netw.*, vol. 4, no. 11, pp. 737–758, Nov. 2005.
- [33] Y.-S. Liao, H.-C. Kuo, Y.-J. Chen, and G.-R. Lin, "Side-mode transmission diagnosis of a multichannel selectable injection-locked Fabry-Perot laser diode with anti-reflection coated front facet," *Opt. Commun.*, vol. 17, no. 6, pp. 4859–4867, Mar. 2009.
- [34] G.-R. Lin, Y.-H. Lin, C.-J. Lin, Y.-C. Chi, and G.-C. Lin, "Reusing a data-erased ASE carrier in a weak-resonant-cavity laser diode for noise-suppressed error-free transmission," *IEEE J. Quantum Electron.*, vol. 47, no. 5, pp. 676–685, May 2011.
- [35] T. T. Shih, P. H. Tseng, Y. Y. Lai, and W. H. Cheng, "Compact TO-CAN header with bandwidth excess 40 GHz," *J. Lightw. Technol.*, vol. 29, no. 17, pp. 2538–2544, Sep. 2011.
- [36] Y.-C. Chi, Y.-C. Li, and G.-R. Lin, "Specific jacket SMA connected TO-can package FPLD transmitter with direct modulation bandwidth beyond 6 GHz for 256-QAM single or multi-subcarrier OOFDM up to 15Gbit/s," *J. Lightw. Technol.*, vol. 31, no. 1, pp. 28–35, Jan. 2013.
- [37] G.-R. Lin, T.-K. Cheng, Y.-H. Lin, G.-C. Lin, and H.-L. Wang, "Suppressing chirp and power penalty of channelized ASE injection-locked mode-number tunable weak-resonant-cavity FPLD transmitter," *IEEE J. Quantum Electron.*, vol. 45, no. 9, pp. 1106–1113, Sep. 2009.
- [38] G.-R. Lin, T.-K. Cheng, Y.-C. Chi, G.-C. Lin, H.-L. Wang, and Y.-H. Lin, "200-GHz and 50-GHz AWG channelized linewidth dependent transmission of weak-resonant-cavity FPLD injection-locked by spectrally sliced ASE," *Opt. Exp.*, vol. 17, no. 20, pp. 17739–17746, Sep. 2009.
- [39] L. Hanzo, W. Webb, and T. Keller, *Single- and Multi-Carrier Quadrature Amplitude Modulation*, 2nd ed. Chichester, U.K.: Wiley, 2000.
- [40] C.-C. Wei, "Small-signal analysis of OOFDM signal transmission with directly modulated laser and direct detection," *Opt. Lett.*, vol. 36, no. 2, pp. 151–153, Jan. 2011.
- [41] International Telecommunications Union (ITU), "Telecommunications standardization sector of the ITU (ITU-T)," ITU-T Recommendation G.975.1—Forward Error Correction for High Bit-Rate DWDM Submarine Systems. Geneva, Switzerland, 2004.
- [42] I. B. Djordjevic, M. Arabaci, and L. L. Minkov, "Next generation FEC for high-capacity communication in optical transport networks," *J. Lightw. Technol.*, vol. 27, no. 16, pp. 3518–3530, Aug. 2009.
- [43] Y.-C. Chang, Y.-H. Lin, J.-H. Chen, and G.-R. Lin, "All-optical NRZ-to-PRZ format transformer with an injection-locked Fabry-Perot laser diode at unlasing condition," *Opt. Exp.*, vol. 12, no. 19, pp. 4449–4456, Sep. 2004.
- [44] G.-R. Lin, Y.-H. Lin, and Y.-C. Chang, "Theory and experiments of a mode-beating noise-suppressed and mutually injection-locked Fabry-Perot laser diode and erbium-doped fiber amplifier link," *IEEE J. Quantum Electron.*, vol. 40, no. 8, pp. 1014–1022, Aug. 2004.

**Gong-Ru Lin** (S'93–M'96–SM'04) received the B.S. degree from the Department of Physics, Soochow University, Taiwan, in 1988, the M.S. degree from the Institute of Electro-Optical Engineering, National Chiao Tung University, Taiwan, in 1990, and the Ph.D. degree from the Institute of Electro-Optical Engineering, National Chiao Tung University, Taiwan, in 1996.

He has been engaged with several universities in Taiwan from 1997–2006, and has promoted as associated professor in 2001 and full professor in 2004. Since 2006, He directs the Laboratory of Fiber Laser Communications and Si Nano-Photonics with the Graduate Institute of Photonics and Optoelectronics in National Taiwan University. He has a broadband research spectrum covering the fiber-optical communications, the femtosecond mode-locked fiber lasers, the all-optical data processing, the nanocrystallite Si photonics, and the millimeter-wave photonic phase-locked loops.

Dr. Lin is the Senior Member of OSA, a Fellow of SPIE, the Fellow of IET, and the Fellow of IOP. He serves as the Chair of IEEE Photonics Society Taipei Chapter from 2008–2011.

**Yu-Chieh Chi** was born in Taipei, Taiwan, in 1983. He received the B.S. degree from the Department of Electrical Engineering (EE), National Taipei University of Technology (NTUT), Taiwan, in 2005, the M.S. degree from Department of Electro-Optical Engineering, NTUT, and the Ph.D. degree from the Graduate Institute of Photonics and Optoelectronics at National Taiwan University (NTU), Taipei, Taiwan, in 2012.

His research interests are semiconductor laser diodes and optical amplifiers, and their application in fiber-optic communication networks with different architectures including WDM, TDM, PSK and OFDM.

**Yi-Cheng Li** was born in Taipei, Taiwan, in 1988. He received the B.S. degree in engineering science and science engineering from National Taiwan University (NTU), Taiwan, in 2011 and he currently working toward the M.S. degree at the Graduate Institute of Photonics and Optoelectronics, NTU, Taipei, Taiwan.

He has studied ship building and organic material. His researching interests include fiber-optic communications, laser device material and communication system formats.

**Jyehong (Jason) Chen** received the B.S. and M.S. degrees in electrical engineering from National Taiwan University, Taiwan, in 1988 and 1990, respectively, and the Ph.D. degree in electrical engineering and computer science from the University of Maryland Baltimore County, Baltimore, MD, USA, in 1998.

In 1998, he joined the JDSU Uniphase Corporation, as a Senior Engineer. In 2003, he joined the faculty of National Chiao Tung University, Hsinchu, Taiwan, where he is currently an Associate Professor with the Institute of Electro-Optical Engineering and the Department of Photonics. He holds ten U.S. patents (earned within a two-year period).